J Therm Anal Calorim (2016) 124:1341–1347
DOI 10.1007/s10973-016-5298-9

First-principles study for thermodynamic properties of wurtzite indium pnictides

Shweta D. Dabhi[1] · **Prafulla K. Jha**[2]

Received: 31 August 2015 / Accepted: 23 January 2016 / Published online: 8 February 2016

Abstract The results of the thermodynamical functions such as lattice specific heat at constant volume, entropy, Debye temperature, internal energy and vibrational free energy with temperature are presented to understand the thermal behaviour and performance of three indium pnictide compounds in wurtzite phase. We have used a first-principles method based on density functional theory and quasi-harmonic approximation. Phonon dispersion curves show no imaginary frequency for any phonon modes throughout the Brillouin zone which confirms the dynamical stability of these compounds in wurtzite phase. Our calculated vibrational frequency matches well with experimental Raman spectra of corresponding wurtzite nanowires. Internal energy and vibrational contribution of Helmholtz free energy, respectively, increases and decreases with temperature. An increase with temperature is observed for entropy. The variation of specific heat at constant volume and Debye temperature is also presented and correlated with speed of phonons and phonon mean free path. The characteristic features of temperature variation of considered thermodynamic functions are in line with those of other crystalline semiconductors.

Keywords Ab initio · Indium pnictide · Thermal properties · Lattice dynamics

✉ Prafulla K. Jha
prafullaj@yahoo.com

[1] Department of Physics, Maharaja Krishnakumarsinhji Bhavnagar University, Bhavnagar 364001, India

[2] Department of Physics, Faculty of Science, The M. S. University of Baroda, Vadodara 390002, India

Introduction

The III–V semiconducting materials like InP, InAs and InSb in both bulk and nanoforms have always been considered as important materials from the fundamental [1, 2] as well as technological [3–7] point of view due to their great promise for a range of applications including field effect transistors [6, 8], photodetectors [9], thermoelectric [10] and solar cells [11]. These applications are based on a large number of desirable properties such as vibrational, thermal conductivity, high electron mobility and direct band gap. These materials generally have a typical cubic zinc blende (ZB-3C) crystal structure at ambient conditions in bulk form [12]. However, recently it has been shown that these compounds can also be grown in other crystal phases that are not possible in bulk form such as wurtzite (WZ) 2H, 4H and 6H polytypes [13–16].

The discovery of WZ phase in addition to the cubic ZB phase opens the new way to novel physics and ideas for nanostructure applications due to the variation of the electronic structure with the crystal structure [17]. Further, the ability to tune the crystal phases during nanowire growth can lead to many important implications for the phonon-related properties such as thermal conductivity, entropy and specific heat of nanostructure [18–22]. The phase-specific properties are relevant in many applications. Motivated with this fact, the electronic band structure of some of the WZ III–V semiconductor compounds [23] and pressure-dependent Raman spectra together with the phonon dispersion curves (PDC) have been reported for WZ-InAs [18–20]. The literature reveals a significant amount of work from both theory and experiment mainly focusing on investigating the electronic and vibrational properties of group III pnictides in WZ phase [18–23]. However, very little effort has been made to analyse the thermal properties of bulk InP, InAs and InSb in WZ phase.

In this work, we report a systematic theoretical investigation of vibrational and thermodynamical properties of bulk InP, InAs and InSb in WZ phase using first-principles calculations and quasi-harmonic approximation (QHA). We have used the density functional theory to calculate the total energy for equilibrium crystal structures and to compute phonon density of states (PhDOS) which is an important ingredient required for the calculation of thermodynamical functions from first principles [24–28]. The calculation of PhDOS is not only essential for the calculation of thermodynamic functions but also a real test of the used methodology to obtain phonon modes as it requires the calculation of PDC in entire Brillouin zone (BZ).

Computational methods

First-principles calculations based on density functional theory for indium pnictides in WZ phase have been performed using Quantum Espresso code [29] which uses self-consistent field approach using plane-wave basis set to compute the total energies. The local density approximation (LDA) to exchange correlation functional of Perdew and Zunger type [30] is used in the present calculations. Previous studies confirm that the LDA does a better job than generalized gradient approximation (GGA) for III–V compounds [31]. Monkhorst and Pack k-points grid of $16 \times 16 \times 10$ is used to sample the BZ. Density functional perturbation theory (DFPT) developed by Baroni et al. [24] is utilized to get full PDC and PhDOS. We have used the $4 \times 4 \times 3$ q-mesh in the first BZ to interpolate the force constants for the phonon dispersion calculations. Thermal properties are calculated using QHA [24] and PhDOS is obtained by DFPT. Thermodynamic functions such as constant volume specific heat (C_v), entropy (S), internal energy ΔE and vibrational part of Helmholtz free energy ΔF are calculated using relations described in [24] and useful for variety of systems [25, 26].

Results and discussion

Structural properties

To calculate the thermodynamical functions of WZ-InX (X = P, As and Sb), we first optimized the crystal structure and lattice parameter and used them to calculate PDC and PhDOS from which thermal properties can be derived. The calculated ground-state properties such as lattice parameters, bulk modulus and derivative of bulk modulus with respect to pressure B_0' are obtained using the above-discussed method and listed in Table 1 along with available experimental and other theoretical data [13, 22, 32–36] for the comparison. The bulk modulus and its pressure derivative for these compounds have been found by minimizing the total energy for the different values of lattice parameter using Murnaghan equation of state and compared with available theoretical data. First derivative of bulk modulus with respect to pressure (dB_0/dP) has expected value around four for all three WZ indium pnictide compounds.

As bulk InX is synthesized in ZB phase only and WZ phase is observed for InX nanosystems (nanowires and nanowhiskers), there exist few studies for thermodynamical properties of these compounds mainly concentrating on ZB phase [37]. As there is a large difference observed for various properties depending on the structural difference of

Table 1 Lattice parameter, bulk modulus and its pressure derivative with available experimental and other theoretical data

Reference	Lattice parameter a/Å [c/a]	Bulk modulus B_0/GPa	Pressure derivative of Bulk modulus B_0'
InP			
Present calc	4.0858 [1.639]	74.1	4.63
Experiment	4.1423 [1.6419][a]		
Other calc	4.1148 [1.6408][b], 4.1215 [1.6432][e]	71.2[b], 60.88[f], 73.06[g]	5.195[f], 4.49[g]
InAs			
Present calc	4.2175 [1.638]	62.9	4.38
Experiment	4.2742 [1.643][c]		
Other calc	4.2108 [1.6412][d], 4.192 [1.6326][g]	61.9[b], 60.98[g]	4.57[g]
InSb			
Present calc	4.507 [1.645]	48.5	4.59
Experiment	4.5712 [1.6455][c]		
Other calc	4.5547 [1.6424][b], 4.494 [1.6326][g]	46.9[b], 46.9[g]	4.68[g]

[a] [32], [b] [13], [c] [33], [d] [22], [e] [34], [f] [35], [g] [36]

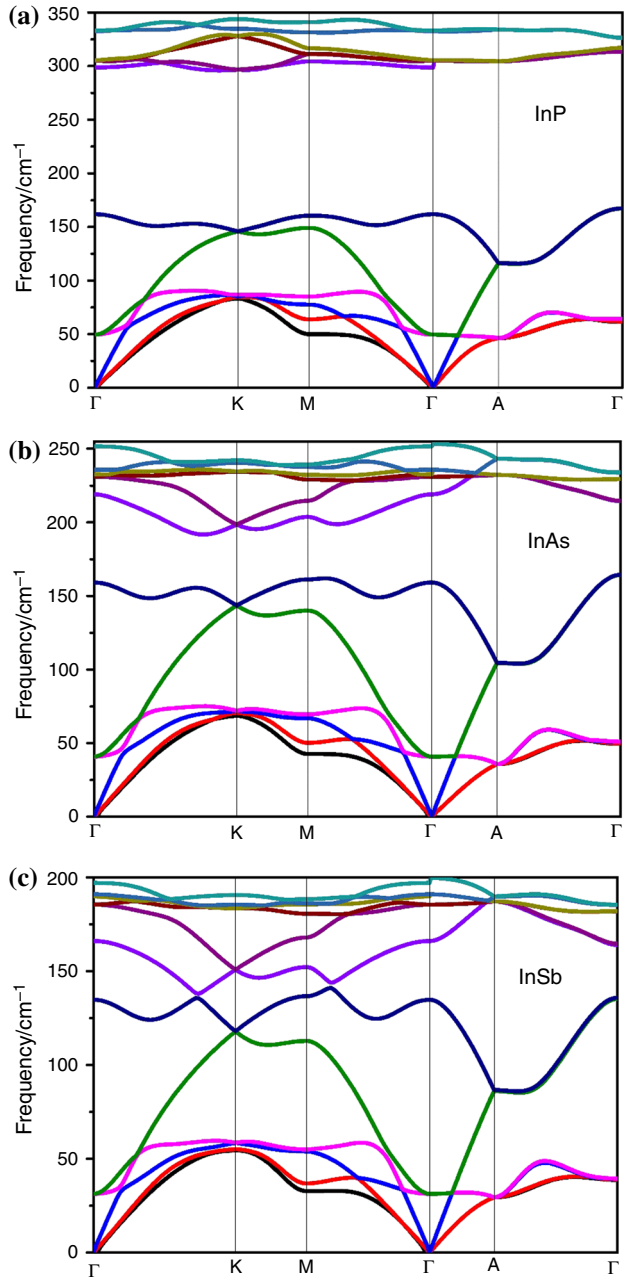

Fig. 1 Phonon dispersion curves of wurtzite (**a**) InP, (**b**) InAs and (**c**) InSb

ZB and WZ forms in III–V semiconductor systems [38], we carried out ab initio calculation for vibrational and thermal properties of InX in WZ phase.

Vibrational properties

Now we turn our focus on the phonon properties of three III–V compounds, viz. InP, InAs and InSb in WZ phase, using theoretically obtained equilibrium structural parameters. Figure 1a–c presents the PDC for WZ-InX. Since there is no experimental data on PDC available for these compounds in WZ phase, we could not compare our PDC with experimental data. However, in Table 2, we present our calculated Raman frequencies and compare them with the available experimental and theoretical data for WZ-InX [18, 19, 34, 39, 40]. As mentioned earlier, WZ phase is yet not observed in bulk phase, so we have compared theoretically obtained Raman frequencies of WZ-InX in bulk form with experimentally synthesized WZ-InX in nanowire form. As observed from Table 2, going from indium phosphide to antimonide, the frequency of Raman modes decreases with the increase in atomic mass of pnictide atoms. Further, Fig. 1 depicts that the PDC calculated for WZ-InX agree quite well with the other available theoretical PDC [22, 34]. Figure 1 also reveals that the frequency of all phonon modes in PDC is positive throughout the BZ which indicates that the InP, InAs and InSb in WZ phase is dynamically stable. There are twelve phonon branches in full PDC since the unit cell of WZ-InX has four atoms. The LO-TO splitting decreases as going from phosphide to antimonide. Maximum frequency observed for optical phonon branches also decrease as going from InP to InSb (from 350 to 200 cm^{-1}).

The PhDOS presented in Fig. 2 for all three compounds reflect all important features of PDC. Further, the PhDOS which is an essential quantity to calculate the thermodynamical functions is also a real test of any theoretical calculation as it requires the calculation of phonon modes in entire BZ [41–44]. Figures 1a and 2a show that a large gap between the acoustic and optical phonon branches is formed in the WZ-InP due to large mass difference between In and P atoms which reduces going from WZ-InP to InAs, and finally in case of InSb, no separation is observed in Figs. 1c and 2c due to overlapping of acoustic and optical branches.

Thermal properties

To have an insight into the thermal behaviour of InP, InAs and InSb in WZ phase, we have investigated the temperature-dependent thermodynamical functions, viz. specific heat at constant volume (C_v), entropy (S), internal energy (ΔE) and vibrational free energy (ΔF), using methodology discussed in Sect. 2. Specific heat capacity together with Debye temperature characterizes the thermodynamic features of a crystalline structural material.

Figure 3a–d presents the thermodynamic functions such as specific heat at constant volume, entropy, internal energy and vibrational free energy with temperature for three indium pnictide compounds in WZ phase. Figure 3a illustrates computed temperature dependence of lattice specific heat at constant volume which clearly reveals that the specific heat behaviour approaches the Dulong and

Table 2 Raman frequencies for indium pnictide compounds in wurtzite form

Mode	InP		InAs		InSb	
	Present	Other	Present	Other	Present	Other
A_1 (TO)	299.5	304.6[a], 302.1[b]	232.6	–	166.5	145[e]
E_1 (TO)	305.1	309.2[a], 302.4[b]	219.4	219.3[c], 215.5[d]	–	–
E_{2h}	305.4	307.9[a], 306.4[b]	229.9	214.1[c], 214.6[d]	184.7	180[e]
A_1 (LO)	332.8	340.2[a], 341.9[b]	236.1	240[c], 239.3[d]	189.8	–
E_1 (LO)	334.4	339.1[a]	252.1	–	191.1	230[e]

[a] [34], [b] [39], [c] [18], [d] [19], [e] [40]

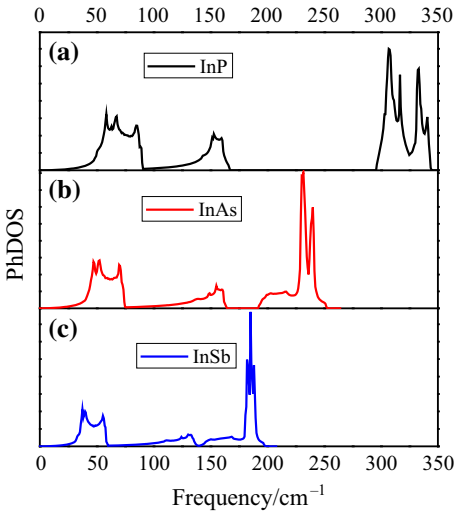

Fig. 2 Phonon density of states of wurtzite (**a**) InP, (**b**) InAs and (**c**) InSb

Petit limit at high temperature. For WZ-InX compounds, Dulong and Petit value ($3N_AK_B$: N_A is Avogadro constant, and K_B is Boltzmann constant) is $\approx 3R$ (where R is gas constant) that is consistent with the nature of the solid in high-temperature region. At very low temperatures, the relation between specific heat capacity and temperature follows Debye T^3 law arising mainly due to long wavelength acoustical phonons. The lattice specific heat at constant volume is lowest for WZ-InP and highest for WZ-InSb among three considered indium pnictides. The computed temperature variation of phonon contribution to entropy which is presented in Fig. 3b reveals that the entropy increases with temperature. The entropy S, an extensive state function accounting the effects of irreversibility in thermodynamic states and a measure of disorder at molecular level, is an important quantity in thermodynamics. Entropy values at different temperature follow the relations InP < InAs < InSb in WZ phase of indium pnictides. At low temperature, internal energy is scarce due to less vibrations of atoms owing to their low thermal energy. Figure 3c and d show behaviour of internal energy and vibrational free energy, respectively, with temperature for all three WZ-InX compounds. It is clear from Fig. 3c that the internal energy is highest for WZ-InP than WZ-InAs and WZ-InSb and it increases continuously with temperature. Figure 3d represents the vibrational free energy which is actually vibrational contribution of Helmholtz free energy at different temperatures which reveals that the free energy decreases with temperature in all cases. The zero temperature value of vibrational free energy ΔF_0 and internal energy ΔE_0 becomes equal and does not vanish due to the zero point vibration which can be calculated from the asymptotic expression of respective quantities. Our calculated value of ΔF_0 and ΔE_0 is 12.01, 8.45 and 6.81 mRy, respectively, for WZ-InP, InAs and InSb. These thermodynamical functions follow general trends with temperature as observed for other nitride compounds calculated using density functional theory [25, 26].

It is to be noted that the trends for the thermal properties obtained in the present case are similar to their behaviour in ZB phase of these compounds [37]. However, the difference in the magnitude of these quantities can be attributed to the difference in phonon frequencies. In Table 2, we compare the calculated entropy of InX compounds in the WZ phase with experimental [45] as well as theoretical data [37]. As WZ phase contains four atoms per unit cell while ZB phase contains two atoms per unit cell, we have normalized entropy per atom accordingly. Table 3 clearly shows a small difference in the entropy per atom of these compounds in both the phases. This is quite obvious as no significant change in the group velocity is observed for the acoustic branches in the case of these compounds existing in both the phases [22]. The similar quantity the speed of sound in WZ-InAs nanowire and bulk ZB-InAs is also same [46]. Similarly, the specific heat for AlN and GaN in both WZ and ZB phases is also equal [47]. These can be

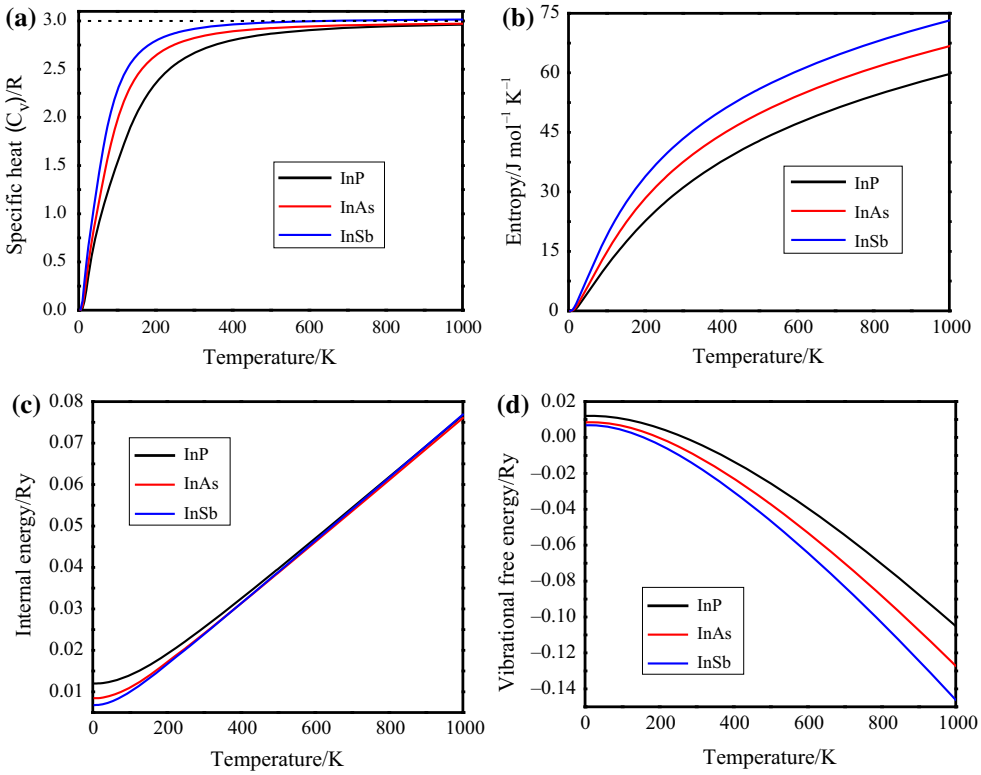

Fig. 3 Specific heat at constant volume, entropy, internal energy and vibrational free energy of WZ-InX (X = P, As and Sb) as a function of temperature

Table 3 Entropy per atom (in unit of J/mol K) in WZ (present calculation) and ZB phase

Temp/K	InP		InAs		InSb	
	WZ	ZB	WZ	ZB	WZ	ZB
295	30.629	31.70[a], 29.90[b]	37.058	38.59[a], 37.85[b]	42.915	43.84[a], 43.09[b]
300	31.000	31.84[a], 30.04[b]	37.452	38.74[a], 37.99[b]	43.323	43.99[a], 43.25[b]
400	37.551	38.47[a], 36.68[b]	44.294	45.65[a], 44.92[b]	50.362	50.99[a], 50.55[b]
500	42.813	43.77[a], 41.99[b]	49.693	51.09[a], 50.38[b]	55.881	56.48[a], 56.42[b]
600	47.190	48.18[a], 46.47[b]	54.143	55.58[a], 54.91[b]	60.416	60.99[a], 61.31[b]
700	50.929	51.93[a], 50.37[b]	57.924	59.38[a], 58.79[b]	64.263	64.81[a], 65.53[b]
800	54.190	55.21[a], 53.84[b]	61.209	62.68[a], 62.21[b]	67.601	
900	57.078	58.11[a], 56.99[b]	64.114	65.61[a], 65.27[b]	70.549	
1000	59.670		66.715	68.22[a], 68.04[b]	73.189	

[a] [34], [b] [41]

finally attributed to the close match of phonon behaviour in (Γ-A) and (Γ-L) directions of WZ and ZB phase, respectively, [22].

Figure 4 presents the calculated temperature variation of Debye temperature (Θ_D) for three WZ-InX compounds: InP, InAs and InSb. Θ_D value at $T \rightarrow 0$ for InP, InAs and InSb is 268, 231 and 189 K, respectively, which shows a decreasing trend as going from phosphide to antimonide. The minimum value of Debye temperature, $\Theta_{D\text{-min}}$ (at Temperature), is 204 K (17 K), 168 K (15 K) and 133 K (11 K) for InP, InAs and InSb, respectively. It is observed from the figure that there is a rapid increase in Debye temperature after $\Theta_{D\text{-min}}$. This can be attributed to the higher phonon transfer speed and mean free path in these systems. The stability (with very small dispersion) in the Debye temperature and specific heat at higher temperatures is due to the stability in phonon mean free path at temperature above 150 K.

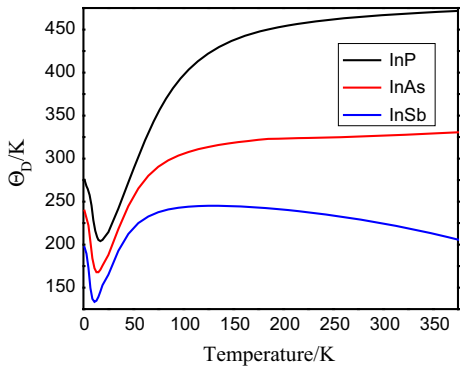

Fig. 4 Debye temperature of WZ-InX (X = P, As and Sb) as a function of temperature

Conclusions

Thermodynamic functions of three indium pnictide compounds in a new WZ phase normally observed in the nanostructure materials are determined by first-principles calculations based on DFPT and QHA. The calculated PDC show no imaginary frequency in entire BZ confirming the dynamical stability of indium pnictides in WZ phase. Optical phonon frequencies match well with available Raman spectra of WZ-InX in nanowire form. The temperature dependence of thermodynamic properties such as specific heat at constant volume, internal energy, vibrational free energy and entropy are investigated and discussed. Specific heat capacity at constant volume obeys Debye T^3 law at low temperature and tends to the Dulong–Petit limit at high temperature. The Debye temperature increases almost slowly with the rise of temperature which is attributed to the decrease in phonon mean free path and phonon transfer speed.

Acknowledgements Work is supported by Science and Engineering Research Board of Govt. of India, Department of Science and Technology (DST) and University Grants Commission, New Delhi, India. SD is grateful to DST for senior research fellowship under INSPIRE scheme.

References

1. Assali S, Zardo I, Plissard S, Kriegner D, Verheijen MA, Bauer G, Meijerink A, Belabbes A, Bechstedt F, Haverkort JEM, Bakkers EPAM. Direct band gap wurtzite gallium phosphide nanowires. Nano Lett. 2013;13:1559–63.
2. Mourik V, Zuo K, Frolov SM, Plissard SR, Bakkers EPAM, Kouwenhoven LP. Signatures of Majorana fermions in hybrid superconductor-semiconductor nanowire devices. Science. 2012;336:1003–7.
3. Saxena D, Mokkapati S, Parkinson P, Jiang N, Gao Q, Tan HH, Jagadish C. Optically pumped room-temperature GaAs nanowire lasers. Nat Photon. 2013;7:963–8.
4. Li Y, Qian F, Xiang J, Lieber CM. Nanowire electronic and optoelectronic devices. Mater Today. 2006;9:18–27.
5. Mayer B, Rudolph D, Schnell J, Morkötter S, Winnerl J, Treu J, Müller K, Bracher G, Abstreiter G, Koblmüller G, Finley JJ. Lasing from individual GaAs–AlGaAs core-shell nanowires up to room temperature. Nat Commun. 2013;4:2931.
6. Vitiello MS, Coquillat D, Viti L, Ercolani D, Teppe F, Pitanti A, Beltram F, Sorba L, Knap W, Tredicucci A. Room-temperature terahertz detectors based on semiconductor nanowire field-effect transistors. Nano Lett. 2012;12:96–101.
7. Yan R, Gargas D, Yang P. Nanowire photonics. Nat Photon. 2009;3:569–76.
8. Duan X, Huang Y, Cui Y, Wang J, Lieber CM. Indium phosphide nanowires as building blocks for nanoscale electronic and optoelectronic devices. Nature. 2001;409:66–9.
9. Lohn AJ, Onishi T, Kobayashi NP. Optical properties of indium phosphide nanowire ensembles at various temperatures. Nanotechnology. 2010;21:355702-1–6.
10. Carrete J, Longo RC, Gallego LJ. Prediction of phonon thermal transport in thin GaAs, InAs and InP nanowires by molecular dynamics simulations: influence of the interatomic potential. Nanotechnology. 2011;22:185704-1–6.
11. Wallentin J, Anttu N, Asoli D, Huffman M, Aberg I, Magnusson MH, Siefer G, Fuss-Kailuweit P, Dimroth F, Witzigmann B, Xu HQ, Samuelson L, Deppert K, Borgström MT. InP nanowire array solar cells achieving 13.8 % efficiency by exceeding the ray optics limit. Science. 2013;339:1057–1060.
12. Dick KA, Caroff P, Bolinsson J, Messing ME, Johansson J, Deppert K, Wallenberg LR, Samuelson L. Control of III–V nanowire crystal structure by growth parameter tuning. Semicond Sci Technol. 2010;25:024009.
13. Panse C, Kriegner D, Bechstedt F. Polytypism of GaAs, InP, InAs, and InSb: an ab initio study. Phys Rev. 2011;84:075217.
14. Mikkelsen A, Skold N, Ouattara L, Borgstrom M, Andersen JN, Samuelson L, Seifert W, Lundgren E. Direct imaging of the atomic structure inside a nanowire by scanning tunnelling microscopy. Nat Mater. 2004;3:519–23.
15. Johansson J, Karlsson LS, Patrik C, Svensson T, Martensson T, Wacaser BA, Deppert K, Samuelson L, Seifert W. Structural properties of <111> B-oriented III–V nanowires. Nat Mater. 2006;5:574–80.
16. Hiruma K, Yazawa M, Haraguchi K, Ogawa K, Katsuyama T, Koguchi M, Kakibayashi H. GaAs free-standing quantum-size wires. J Appl Phys. 1993;74:3162–71.
17. Pemasiri K, Montazeri M, Gass R, Smith LM, Jackson HE, Yarrison-Rice J, Paiman S, Gao Q, Tan HH, Jagadish C, Zhang X, Zou J. Carrier dynamics and quantum confinement in type II ZB-WZ InP nanowire homostructures. Nano Lett. 2009;9:648–54.
18. Yazji S, Zardo I, Hertenberger S, Morkötter S, Koblmüller G, Abstreiter G, Postorino P. Pressure dependence of Raman spectrum in InAs nanowires. J Phys Condens Matter. 2014;26:235301.
19. Majumdar D, Basu A, Mukherjee GD, Ercolani D, Sorba L, Singha A. Raman scattering study of InAs nanowires under high pressure. Nanotechnology. 2014;25:465704.
20. Dabhi SD, Jha PK. Phonon dispersion and Raman spectra of wurtzite InAs under pressure. J Phys Chem Solids. 2015;83:70.
21. Petrova NV, Yakovkin IN. DFT calculations of phonons in GaAs with zinc blende and wurtzite structures. Phys Status Solidi B. 2013;250(10):2141–4.
22. Zhou F, Moore AL, Bolinsson J, Persson A, Froberg L, Pettes MT, Kong H, Rabenberg L, Caroff P, Stewart DA, Mingo N, Dick KA, Samuelson L, Linke H, Shi L. Thermal conductivity of indium arsenide nanowires with wurtzite and zinc blende phases. Phys Rev B. 2011;83:205416.

23. De A, Pryor CE. Predicted band structures of III–V semiconductors in the wurtzite phase. Phys Rev B. 2010;81:155210.
24. Baroni S, de Gironcoli S, Corso AD, Giannozzi P. Phonons and related crystal properties from density-functional perturbation theory. Rev Mod Phys. 2001;73:515.
25. Gupta SD, Gupta SK, Jha PK. High pressure study on the phonon spectra and thermal properties in hafnium nitride and zirconium nitride. J Therm Anal Calorim. 2012;107:49–53.
26. Mankad V, Gupta SK, Soni H, Jha PK. Density functional theoretical study of lattice-specific heat and thermal properties of magnesium nitride. J Therm Anal Calorim. 2012;107:45–8.
27. Sedmidubsk D, Leitner J, Svoboda P, Sofer Z, Macháek J. Heat capacity and phonon spectra of $A^{III}N$ experiment and calculation. J Therm Anal Calorim. 2009;2:403–7.
28. Hetmańczyk Ł, Hetmańczyk J. Comparison of vibrational dynamics, thermal behaviour, and phase transition in $[Ni(NH_3)_4](ReO_4)_2$ and $[Ni(NH_3)_6](ReO_4)_2$. J Therm Anal Calorim. 2015;119:1415.
29. Giannozzi P, Baroni S, Bonini N, Calandra M, Car R, Cavazzoni C, Ceresoli D, Chiarotti GL, Cococcioni M, Dabo I, Corso AD, Fabris S, Fratesi G, Gironcoli S, Gebauer R, Gerstmann U, Gougoussis C, Kokalj A, Lazzeri M, Martin-Samos L, Marzari N, Mauri F, Mazzarello R, Paolini S, Pasquarello A, Paulatto L, Sbraccia C, Scandolo S, Sclauzero G, Seitsonen AP, Smogunov A, Umari P, Wentzcovitch RM. QUANTUM ESPRESSO: a modular and open-source software project for quantum simulations of materials. J Phys Condens Matter. 2009;21:395502.
30. Perdew JP, Zunger A. Self-interaction correction to density-functional approximations for many-electron systems. Phys Rev B. 1981;23:5048.
31. Haas P, Tran F, Blaha P. Calculation of the lattice constant of solids with semi local functionals. Phys Rev B. 2009;79:085104-1–-10.
32. Kriegner D, Wintersberger E, Kawaguchi K, Wallentin J, Borgström MT, Stangl J. Unit cell parameters of wurtzite InP nanowires determined by X-ray diffraction. Nanotechnology. 2011;22:425704.
33. Kriegner D, Panse C, Mandl B, Dick KA, Keplinger M, Persson JM, Caroff P, Ercolani D, Sorba L, Bechstedt F, Stangl J, Bauer G. Unit cell structure of crystal polytypes in InAs and InSb nanowires. Nano Lett. 2011;11:1483.
34. Mukhopadhyay S, Stewart DA. First-principles study of the phonon dispersion and dielectric properties of wurtzite InP: role of In 4d electrons. Phys Rev B. 2014;89:054302.
35. Branicio PS, Rino JP, Gan CK, Tsuzuki H. Interaction potential for indium phosphide: a molecular dynamics and first-principles study of the elastic constants, generalized stacking fault and surface energies. J Phys Condens Matter. 2009;21:095002.
36. Wang SQ, Ye HQ. A plane-wave pseudopotential study on III–V zinc-blende and wurtzite semiconductors under pressure. J Phys Condens Matter. 2002;14:9579–87.
37. Hou HJ, Kong FJ. Theoretical investigation on the structural, dynamical, and thermodynamic properties of the zinc-blende InX (X ¼ P, As, Sb). Phys Status Solidi B. 2011;248(6):1399–404.
38. Farahmand M, Brennan KF. Comparison between wurtzite phase and zinc blende phase GaN MOSFETs using a full band Monte Carlo simulation. IEEE Trans Electron Devices. 2000;47:493–7.
39. Gadret EG, Lima MM Jr, Madureira JR, Chiaramonte T, Cotta MA, Iikawa F, Cantarero A. Optical phonon modes of wurtzite InP. Appl Phys Lett. 2013;102:122101.
40. Pizani PS, Jasinevicius RG. The effect of high non-hydrostatic pressure on III–V semiconductors: zinc blende to wurtzite structural phase transition and multiphase generation. J Phys Conf Ser. 2014;500:182032.
41. Jha PK, Sanyal SP. Phonon spectrum and lattice specific heat of the $HgBa_2CuO_4$ high-temperature superconductor. Phys C. 1996;271:6–10.
42. Jha PK, Sanyal SP. A lattice dynamical study of the role of pressure on Raman modes in high-T_c $HgBa_2CuO_4$. Phys C. 1996;261:259–62.
43. Jha PK. Phonon spectra and vibrational mode instability of $MgCNi_3$. Phys Rev B. 2005;72:214502–6.
44. Jha PK, Sanyal SP. Lattice Vibrations in Yb-pnictide compounds. Phys Rev B. 1995;52(22):15898.
45. Barin I. Thermochemical data of pure substances. 3rd ed. New York: VCH; 1995.
46. Mariager SO, Khakhulin D, Lemke HT, Kjær KS, Guerin L, Nuccio L, Sørensen CB, Nielsen MM, Feidenhans'l R. Direct observation of acoustic oscillations in InAs nanowires. Nano Lett. 2010;10:2461–5.
47. AlShaikhi A, Srivastava GP. Specific heat calculations of III-N bulk materials. Phys Status Solidi C. 2006;3:1495.